Al-Rafidain J Med Sci. 2025;8(2):202-214.
DOI: https://doi.org/10.54133/ajms.v8i2.2047

AJMS

Online ISSN (2789-3219)

Research Article

Wound Healing Effects of Zofenopril and Fisetin in Rat Model of Diabetic Foot Ulcers

Sozan Kamaran AbdulRazaaq, Bushra Hassan Marouf*
Department of Pharmacology and Toxicology, College of Pharmacy, University of Sulaimani, Sulaimani, Kurdistan Region, Iraq

Received: 5 May 2025; Revised: 8 June 2025; Accepted: 11 June 2025

Abstract

Background: Diabetic foot ulcer (DFU) is a prevalent complication of diabetes. Current therapeutic options remain inadequate in controlling its progression. ***Objectives***: To evaluate the wound-healing potential of zofenopril (ZOF) and fisetin (FS) in a rat model of DFU. ***Methods***: Sixty-five rats were included in the study and divided into 7 groups: nDnW: non-diabetic, non-wounded; nDW: non-diabetic, wounded; DWC: diabetic, wounded control. Insulin, ZOF, FS, and ZOF+FS. Diabetes was induced using 60mg/kg streptozotocin (STZ), and a full-thickness excision wound was created on the dorsal surface of the hind paw. The wound size was measured by ImitoWound application. Assessment of blood glucose, C-reactive protein (CRP), interleukin-(IL)-10, total antioxidant capacity (TAOC), vascular endothelial growth factor (VEGF), and hydroxyproline was performed. Tissue samples were examined for histological changes. ***Results***: ZOF, FS, and their combination significantly accelerated diabetic wound healing via reducing wound surface area and percentage of wound contraction, improved glycemic control, and mitigated histological alterations. They significantly reduced the serum level of CRP in the inflammatory phase and increased VEGF and hydroxyproline. Histopathological analysis revealed a reduction in inflammatory infiltration at the wound site, marked angiogenesis and fibroblast proliferation on Day 8, and moderate to excellent epidermal thickness with optimal collagen deposition on Day 16 post-wounding. ***Conclusions***: ZOF, FS, and their combination enhanced wound healing by ameliorating inflammation, improving angiogenesis, collagen synthesis, and re-epithelization. The suggested mechanisms are anti-inflammatory, elevation of the level of VEGF and hydroxyproline, and glycemic control, thereby accelerating wound contraction and improving delayed wound healing in diabetes.

Keywords: Diabetic foot ulcer, Fisetin, Sulfhydrylated ACE-inhibitors, Wound healing, Zofenopril.

آثار التئام الجروح باستخدام زوفينوبريل وفيسيتين في نموذج الجرذان لقرحة القدم السكرية

الخلاصة

الخلفية: قرحة القدم السكرية (DFU) هي أحد المضاعفات السائدة لمرض السكري. لا تزال الخيارات العلاجية الحالية غير كافية للتحكم في تقدمه. **الأهداف**: تقييم إمكانات التئام الجروح لزوفينوبريل (ZOF) وفيسيتين (FS) في نموذج الفئران من DFU.**الطرائق**: تم تضمين خمسة وستين فأرا في الدراسة وتم تقسيمها إلى 7 مجموعات: nDnW: غير مصابين بالسكري، غير مصابين؛ nDW: غير مصابين بالسكري، جرحى. DWC: مجموعة القياس لمرضى السكري والجرحى. الأنسولين و ZOF و FS، و ZOF + FS. تم إحداث مرض السكري باستخدام 60 مجم / كجم من الستربتوزوتوسين (STZ) ، وتم إنشاء جرح استئصال كامل السماكة على السطح الظهري للمخلب الخلفي. تم قياس حجم الجرح بواسطة تطبيق ImitoWound. تم إجراء تقييم نسبة الجلوكوز في الدم، والبروتين التفاعلي C (CRP)، والإنترلوكين 10- (IL)، والقدرة الإجمالية لمضادات الأكسدة (TAOC)، وعامل النمو البطاني الوعائي (VEGF)، وهيدروكسي برولين. تم فحص عينات الأنسجة بحثا عن التغيرات النسيجية. **النتائج**: أدى ZOF و FS ومزيجهما إلى تسريع التئام الجروح السكرية بشكل كبير عن طريق تقليل مساحة سطح الجرح والنسبة المئوية لتقلص الجرح، وتحسين التحكم في نسبة السكر في الدم، وتخفيف التغيرات النسيجية. لقد خفضوا بشكل كبير من مستوى مصل CRP في المرحلة الالتهابية وزادوا من VEGF وهيدروكسي برولين. كشف التحليل النسيجي المرضي عن انخفاض في التسلل الالتهابي في موقع الجرح، وتكوين الأوعية الدموية الملحوظ وانتشار الخلايا الليفية في اليوم 8، وسمك البشرة المعتدل إلى الممتاز مع ترسب الكولاجين الأمثل في اليوم 16 بعد الجرح. **الاستنتاجات**: عززت ZOF و FS ومزيجها التئام الجروح عن طريق تخفيف الالتهاب وتحسين تكوين الأوعية الدموية وتخليق الكولاجين وإعادة الظهارة. الآليات المقترحة هي مضادة للالتهابات، ورفع مستوى VEGF وهيدروكسي برولين، والتحكم في نسبة السكر في الدم ، وبالتالي تسريع تقلص الجروح وتحسين تأخر التئام الجروح في مرض السكري.

* ***Corresponding author***: Bushra H. Marouf, Department of Pharmacology and Toxicology, College of Pharmacy, University of Sulaimani, Sulaimani, Kurdistan Region, Iraq; Email: bushra.marouf@univsul.edu.iq
Article citation: AbdulRazaaq SK, Marouf BH. Wound Healing Effects of Zofenopril and Fisetin in Rat Model of Diabetic Foot Ulcers. *Al-Rafidain J Med Sci*. 2025;8(2):202-214. doi: https://doi.org/10.54133/ajms.v8i2.2047

INTRODUCTION

Wound healing is a multifaceted physiological process that occurs through a series of overlapping phases following tissue injury. It begins with hemostasis and coagulation and progresses to inflammation, proliferation, and remodeling [1]. This complex process is highly governed by a range of growth factors, cytokines, and signals from the extracellular matrix. Different cells, including endothelial cells, fibroblasts, and neutrophils, are important in facilitating wound healing. Ultimately, this process commonly contributes to the creation of scar tissue [2]. In diabetic patients, the healing process is often delayed and can lead to the development of diabetic foot ulcers (DFU). Factors that delay wound healing are increased blood glucose, delayed inflammatory response, elevated oxidative stress, impaired blood supply to the wound site, decreased granulation tissue formation, increased blood

viscosity, increased insulin resistance, reduced angiogenesis, and collagen deposition. Furthermore, inflammatory infiltration and the balance of pro-inflammatory cytokines are crucial in DFU development. Additionally, high blood glucose levels inactivate hypoxia-inducible factor-1 a (HIF-1α), inhibiting vascular endothelial growth factor (VEGF) and endothelial nitric oxide synthase (eNOS) production, thereby hindering diabetic wound healing [3]. VEGF has been shown to stimulate fibroblast proliferation, promoting wound healing through enhanced collagen production [4]. However, in diabetic conditions, poor vasculature at the wound site leads to increased synthesis of inflammatory cytokines, which suppress VEGF-dependent collagen synthesis, thereby delaying wound healing [5]. Hydroxyproline, a non-essential amino acid, plays a crucial role in the formation of the extracellular matrix. Increased hydroxyproline production is considered a key indicator of collagen synthesis, the rate of wound contraction is closely tied to collagen formation and maturation [6]. Studies indicate that the skin's local renin-angiotensin system (RAS) plays an important role in regulating skin functions and is involved in skin physiology and pathophysiology such as wound healing and DFUs, fibrotic disorders, and skin cancers [7]. Angiotensin-converting enzyme (ACE) modulates cutaneous inflammation by degrading neuropeptides like substance P and bradykinin [8]. Numerous studies have shown that angiotensin receptor blockers (ARBs) and ACE inhibitors (ACEIs) have the potential to reduce proinflammatory cytokines and fibrogenic factors, suggesting their therapeutic potential in various skin pathologies [9]. In other words, the tissue RAS plays a role in wound healing and fibrosis, with both pro- and anti-inflammatory effects [10]. Despite the availability of several treatment options for DFU, they are not proving to be adequately effective, and there is a need for more effective treatments to address this serious complication of diabetes. Researchers suggest that ACEIs may enhance glycemic control and insulin sensitivity in diabetic models potentially through increased muscular blood flow, local RAS inhibition, and elevated kinin levels [11]. Both in STZ-diabetic rats and human studies, ACEIs reduced blood glucose levels and boosted peripheral insulin sensitivity [12]. Additionally, the modulation of the RAS by ACEIs has been shown to improve insulin sensitivity, better glycemic control, and the prevention of type 2 diabetes mellitus in various clinical trials [13]. These findings highlight the potential metabolic benefits of ACEIs in diabetes management. On the other hand, the benefits of combining herbal medicine with ACEI/ARB drugs for treating diabetic nephropathy have previously been addressed in the literature [14]. Medicinal plants show promise as adjuvant therapies to conventional wound care for accelerating healing in DFU [15]. Fisetin (FS) (3,7,3',4'-tetrahydroxyflavone) is one of the polyphenolic flavonoids found in various plants such as vegetables and fruits, including cucumbers, onions, strawberries, apples, and persimmons [16]. According to a recent systematic review, FS is indicated as a potent antioxidant among the evaluated flavonoids. It exhibits both direct and indirect antioxidant effects, the latter through the enhancement of reduced glutathione levels and amelioration of oxidative stress in neuronal cells. Fisetin shows significant potential in managing diabetes-related complications [17]. Additionally, it displays anti-inflammatory properties by suppressing NF-κB activity and reducing the production of pro-inflammatory cytokines in hyperglycemic conditions [16]. It also prevents angiogenesis in diabetic retinopathy by downregulating vascular endothelial growth factor (VEGF) [18]. The pleiotropic effects of FS make it a promising candidate for developing effective treatments for diabetic wound healing, and it may be a suitable candidate to synergize the efficacy of RAS inhibitors in the treatment of DFUs. The study aimed to investigate the potential wound-healing effects of zofenopril alone and in combination with fisetin in STZ-induced hyperglycemic rats through assessment of the inflammatory process, oxidative stress status, angiogenesis, collagen synthesis, and histopathological alterations, which are associated with the skin wound in diabetic rats.

METHODS

Drugs and chemicals

Streptozotocin was obtained from MEDIVER, United Kingdom (UK); zofenopril from Mylan, Spain; insulin (Lantus) from Sanofi Aventis, France; pure fisetin 98% from Hansen, Poland; ketamine 10% from Alfasan, Holland; and xylazine 2% injection from Interchemie, Holland. Enzyme-linked immunosorbent assay (ELISA) kits: rat IL-10, VEGF, TAOC, and hydroxyproline from Bioassay Technology Laboratory, UK, and CRP from CRP Industries Inc., USA.

Animals and ethical consideration

This study was carried out on 65 healthy male Wistar albino rats weighing 200±40 g and aged 8-10 weeks, which were supplied by the animal house of the College of Pharmacy-University of Sulaimani. These rats were kept in a clean environment individually in polypropylene cages for one week to acclimatize to the standard laboratory conditions [temperature (25±2ºC), relative humidity (44-56%), and light and dark cycles (12:12 hours)] of a well-ventilated animal house and were free to drink water and eat food. All animal experiments were approved by the Research Registration and Ethics Committee of the College of Pharmacy, University of Sulaimani (Certificate No. PH142-24 on 28th November 2024), and carried out in strict accordance with the Declaration of Helsinki on the welfare of experimental animals [19].

Induction of diabetes and creation of excision wound

Diabetic rats were induced through a single intraperitoneal (IP) injection of streptozotocin (60

mg/kg). This study utilized a pre-established DFU animal model [20]. Briefly, each rat was anesthetized with ketamine (75 mg/kg, IP) and xylazine (10 mg/kg, IP). The wound was created on the dorsal surface of the hind paw of rats in a square pattern marked using a signet marking stamp (designed specifically for this purpose) as previously described with modification [21], and then a layer of skin in full thickness, with a standard area of 4 mm × 4 mm, was removed. The excised skin from each rat was preserved for subsequent histological analysis, serving as samples from day 1 before treatment.

Wound assessment

After the wound has been created, the initial step is to take photographs of the wound using a smartphone and measure the surface area with ImitoWound application. The ImitoWound App was obtained from the Imito company (Imito AG, Flüelastrasse 31, CH-8047 Zürich, Switzerland), which is a precise, standardized, and simple application for digital wound measurement [22]. The package provides the calibration markers, which are necessary to perform measurements. This novel method was validated by a planimetry method of Image J [23].

Experimental design and treatment protocol

The animal groups, treatment protocol, dose, and duration of the experiment are demonstrated in Figure 1. The dose of zofenopril [14,24] and fisetin [25,26] was selected based on the previous studies with modification. Five animals were sequentially euthanized on Day 8 post-wounded and at the end of the experiment, i.e., Day 16, from each group except Group I.

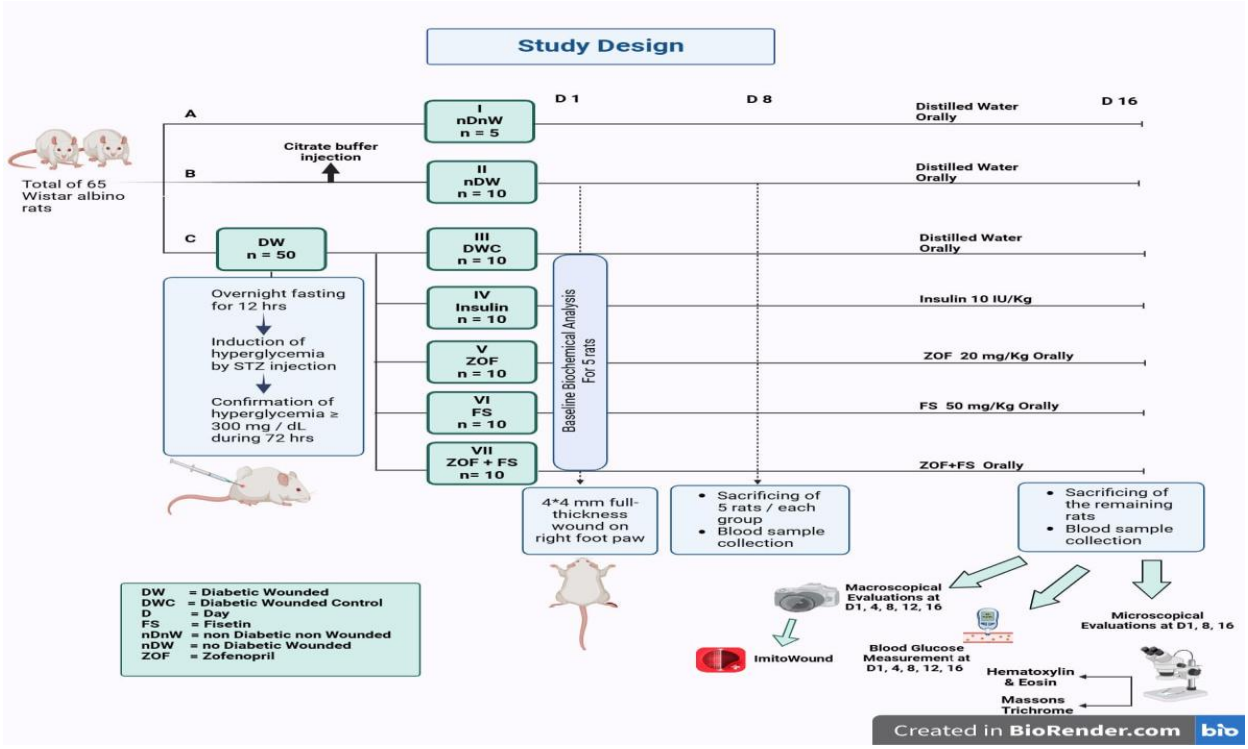

Figure 1: Experimental study design groups and treatment protocols. n: number of animals per group, STZ: streptozotocin.

Blood collection and tissue harvesting

Blood samples were collected from the Caudal Vena Cava on days 8 and 16 following the rat's euthanasia. For measurement of fasting blood glucose levels, the blood was collected from the tail vein on days 1, 8, and 16 of the experiment using an On-Call Plus glucometer from ACON Laboratories, Germany. Five animals of each group were sacrificed sequentially on the 8th and 16th post-wounded days. The fragment of skin surrounding the lesion was placed in 10% formaldehyde for histopathological processing.

Outcome measurement

On Days 1, 4, 8, 12, and 16 post-wounding, photographs with a calibration marker, or ruler, were taken for each wound. The wound area of each animal was measured using the ImitoWound Application. The percentage (%) of wound contraction was calculated by the following formula:

% Wound contraction = 100 * [(Initial wound area) – (nth day wound area)/(Initial wound area)].

Serum levels of IL-10, TAOC, VEGF, and hydroxyproline using an ELISA kit according to the instructions of the detection kit. The CRP was measured by a Cobas c 311 analyzer using a CRP4 kit.

Histopathological analysis

Following humane euthanasia, skin wound samples were collected and processed for histological

preparation. The samples were fixed in 10% neutral buffered formaldehyde for 48 hours. The tissue undergoes dehydration via a sequence of ethanol concentrations (50%, 60%, 70%, 80%, 90%, and 100%), with each interval lasting 1–2 hours, followed by two xylene changes (1–2 hours each) to eliminate the ethanol. The tissue is subsequently infiltrated with molten paraffin wax in an embedding oven at 60°C and embedded in a paraffin block. The paraffin-embedded tissue is sectioned into 5 µm thick slices using a rotary microtome, thereafter, floated in a water bath, and mounted onto glass slides. The slides are dried on a hot plate, deparaffinized in xylene, and rehydrated using a descending series of ethanol concentrations. The sections are stained with Harris's hematoxylin and eosin (H&E), dehydrated, cleaned in xylene, and cover-slipped for microscopic analysis and quantitative assessment. The prepared paraffin-embedded tissue is sectioned into 5 µm thick slices using a rotary microtome, thereafter, floated in a water bath, and mounted onto glass slides. The slides are dried on a hot plate, deparaffinized in xylene, and rehydrated through a descending ethanol series. For Masson's trichrome staining, the sections are first stained with Weigert's iron hematoxylin to highlight nuclei, followed by treatment with Biebrich scarlet acid fuchsin to stain cytoplasm and muscle fibers. The slides are subsequently differentiated in a phosphomolybdic-phosphotungstic acid solution to eliminate excess stain and then dyed with aniline blue to accentuate collagen fibers. Following staining, the slides are rinsed with distilled water, dehydrated using a sequential ethanol series, cleaned with xylene, and then cover-slipped for microscopic analysis. The staining technique facilitates the distinction of collagen (blue), muscle fibers (red), and nuclei (black) in rat foot tissue.

Microscopic quantitative grading

Semiquantitative analysis of wound healing was performed using calibrated Amscope and ImageJ software with high-resolution images captured via a digital microscopic camera. H&E-stained sections were used to assess epidermal thickness, angiogenesis, inflammation, and fibroblast activity, while Masson's trichrome staining quantified collagen on ImageJ. Parameters were evaluated on relevant days. Day 8 for fibroblast proliferation, angiogenesis, and inflammatory cell infiltration, and day 16 for tissue remodeling (collagen deposition). Data from five fields per slide were analyzed using one-way ANOVA (SPSS 23), with significance set at $p<0.05$. Interpretation of scoring and grading for different parameters in wound healing is applied as follows: For epidermal thickness (µm), mean % score 1 if thickness < 4%, 2 if thickness is 4-5%, and 3 if thickness > 5%, with grades excellent, proper, and poor, respectively. For angiogenesis, it means score 1 if <5% angiogenesis, 2 if 5-10% angiogenesis, and 3 if >10% angiogenesis with grades mild, moderate, and marked, respectively. Inflammatory cell infiltration means (%); score 1 if <25% inflammatory cells, 2 if 25-50% inflammatory cells, and 3 if >50% inflammatory cells with grades mild, moderate, and severe, respectively. For fibroblast proliferation, mean (%); 1 if <15% fibroblast proliferation, 2 if 15-25% fibroblast proliferation, and 3 if >25% fibroblast proliferation with grades mild, moderate, and marked, respectively. Collagen deposition means (%); score 1 if <25% collagen deposition, 2 if 25-40% collagen deposition, and 3 if >40% collagen deposition with grades insufficient, moderate, and optimal, respectively.

Ethical consideration

All the procedures in this study followed the standard principle of laboratory animal care and national institutional animal care. Additionally, the protocol of the study was approved by the Ethical and Research Registration Committee of the College of Pharmacy-University of Sulaimani with a registration number (Certificate No. PH42-24 on 28th November 2024).

Statistical analysis

Statistical analysis was performed using GraphPad Prism version 10.4.1 (LLC, CA, USA). Data are presented as mean ± standard error (SEM). The Shapiro-Wilk test was utilized to evaluate the normal distribution of variables. Group differences were analyzed using one-way ANOVA followed by Tukey's test and two-way ANOVA followed by Dunnett's test or Tukey's test. A *p*-value of less than 0.05 was considered statistically significant.

RESULTS

The effects of ZOF and FS and their combination on the body weight of the animals are shown in Figure 2. After diabetic confirmation, the DWC group showed a significant reduction in body weight at each time point, starting from Day 4 and continuing till the end of the experiment, when compared with the nDnW and nDW groups and the baseline (Day 1).

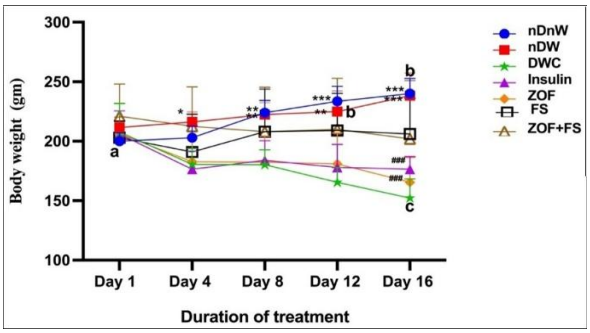

Figure 2: Effect of zofenopril and fisetin alone or in combination on body weight in rats with diabetic foot ulcer. Data presented as mean±SEM, n=5, data analyzed by Two-way ANOVA followed by Dunnett's test. On Day4: **p*= 0.015 when comparing nDW *vs*. DWC, On Day 8: ***p*<0.005 for nDnW and nDW *vs*. DWC. On Day12: ***p*<0.001 for nDW vs DWC, ****p*=0.0001 for nDnW vs DWC, On Day 16: ****p*<0.0002 for nDnW and nDW *vs*. DWC, ### *p*<0.0056 for comparing nDnW and nDW vs. insulin and ZOF. Non-identical letters "a,b,c" indicate significant differences with the baseline day 1. nDnW: non-diabetic, non-wounded; nDW: non-diabetic-wounded; DWC: diabetic wounded control; ZOF: zofenopril; FS: fisetin.

No significant changes in body weight were observed in the rats treated with FS and ZOF+FS. Additionally, rats treated with insulin and ZOF showed a significant reduction in body weight compared to nDnW and nDW, particularly on Day 16 ($p < 0.05$). The effect of ZOF and FS alone or in combination on blood glucose levels in rats with diabetic foot ulcers is shown in Figure 3. On Day 1 of post-diabetic foot wound induction, there was no significant difference in the blood glucose level of nDnW and nDW rats. However, the effect of STZ injection resulted in a significant increase ($p<0.05$) in the blood glucose level of the rats in group DWC compared to the rats in groups nDnW and nDW. However, in the late phases of wound healing, particularly on days 8 and 16, the effects of ZOF, FS, and their combination were comparable and even more effective than insulin in a significant manner ($p < 0.05$). The effect of treatment protocol on wound healing was assessed using a full-thickness hind paw foot ulcer animal model. Animals were treated with insulin, ZOF, and FS individually and with a ZOF+FS combination for 16 days, with wound area measurements recorded on the 1st, 4th, 8th, 12th, and 16th- day post-wounding (Figure 4A and B).

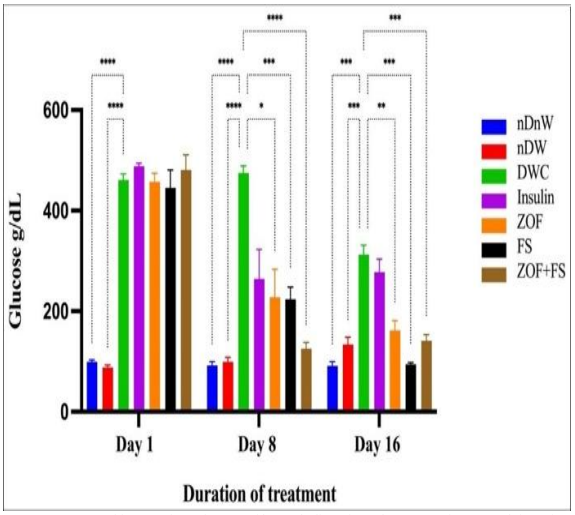

Figure 3: Effect of zofenopril and fisetin alone or in combination on fasting blood glucose in streptozotocin-induced diabetic rats. Data represented as mean ± SEM, n=5, data analyzed by Two-way ANOVA followed by Tukey's test. On Day 1: ****p<0.0001, On Day 8: *p< 0.05, ***p<0.0005, ****p<0.0001, On Day 16: **p<0.003, ***p=0.0007. nDnW: non-diabetic, non-wounded; nDW: non-diabetic-wounded; DWC: diabetic wounded control; ZOF: zofenopril; FS: fisetin.

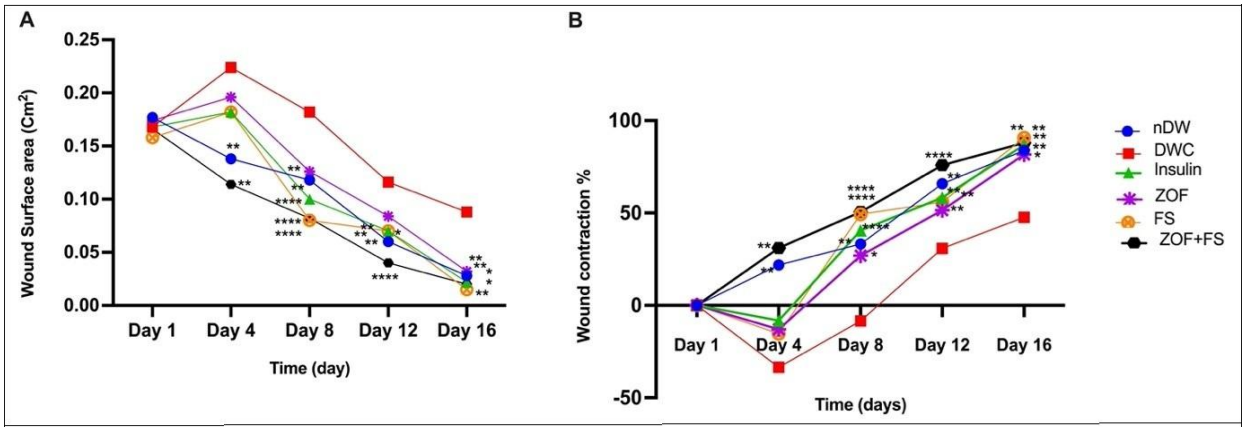

Figure 4: Effect of zofenopril and fisetin alone or in combination on wound surface area and wound contraction percentage in rats with diabetic foot ulcer Data represented as mean ± SEM, number of animals=5, data analyzed by Two-way ANOVA followed by Dunnett's test. **A**) Wound surface area. On Day 4: **p<0.007 when comparing DWC *vs*. nDW, ZOF+FS, On Day 8: **p<0.005 for DWC *vs*. nDW and ZOF, ****p<0.0001 for DWC *vs*. insulin, FS and ZOF+FS, On Day 12: *P<0.02 for DWC vs Insulin, **p<0.002 for DWC *vs*. nDW, ZOF, and FS, ****p<0.0001 for DWC *vs*. ZOF+FS, On Day 16: *p<0.02 for DWC *vs*. nDW and FS, **p<0.005 for DWC *vs*. Insulin, FS and ZOF+FS. **B**) Wound contraction%. On Day 4: **p<0.005 when compare DWC *vs*. nDW, ZOF+FS, On Day 8: *p<0.05 for DWC *vs*. ZOF, **p<0.005 for DWC *vs*. nDW, ****p<0.0001 for DWC *vs*. insulin, FS, and ZOF+FS, On Day 12: **p<0.002 for DWC *vs*. nDW, Insulin, ZOF, and FS, ****p<0.0001 for DWC *vs*. ZOF+FS, On Day 16: *p<0.02 for DWC *vs*. ZOF, **p<0.01 for DWC *vs*. nDW, Insulin, FS and ZOF+FS. nDnW: non-diabetic, non-wounded; nDW: non-diabetic-wounded; DWC: diabetic wounded control; ZOF: zofenopril; FS: fisetin.

In the DWC group, which was treated with only distilled water after STZ injection, the wound surface area was significantly larger ($p < 0.05$) (Figure 4A) than the baseline (Day 1) nDW and ZOF+FS. Insulin treatment (10 IU/kg) significantly reduced ($p < 0.05$) the wound area from day 8, accompanied by a parallel increase in wound contraction rate in a significant manner ($p < 0.05$) compared to the DWC group. Similarly, ZOF, FS, and their combinations significantly ameliorated ($p < 0.05$) STZ-induced changes in wound surface area and percent of wound contraction compared to the DWC group. However, the combination protocol demonstrated a marked ameliorative impact on STZ-induced diabetic foot ulcers compared to the ZOF and FS individually. On day 12 the percentage of wound contraction was markedly higher in the ZOF+FS combination regimen (75.9%) compared to the other treated groups, which were 55.9% for FS, 51.5% for ZOF, and 58.3% for insulin (Figure 4B). Briefly, from the 4th day onward, the combination protocol of ZOF+FS demonstrated an accelerated wound healing process compared to the DWC groups in a statistically significant manner ($p<0.05$). By the 8th, and 12th day, the insulin, ZOF, FS, and ZOF+FS combination demonstrated a significant decrease in the surface area of the wound comparable to the nDW group (Figure 4A). This was achieved by nearly 50% - 80% wound contraction, reaching approximately 100% by the 16th day of the experiment (Figure 4B). Figure 5 demonstrates the effect of ZOF, FS, and their combinations on different phases of wound healing on Days 1, 4, 8, 12, and 16.

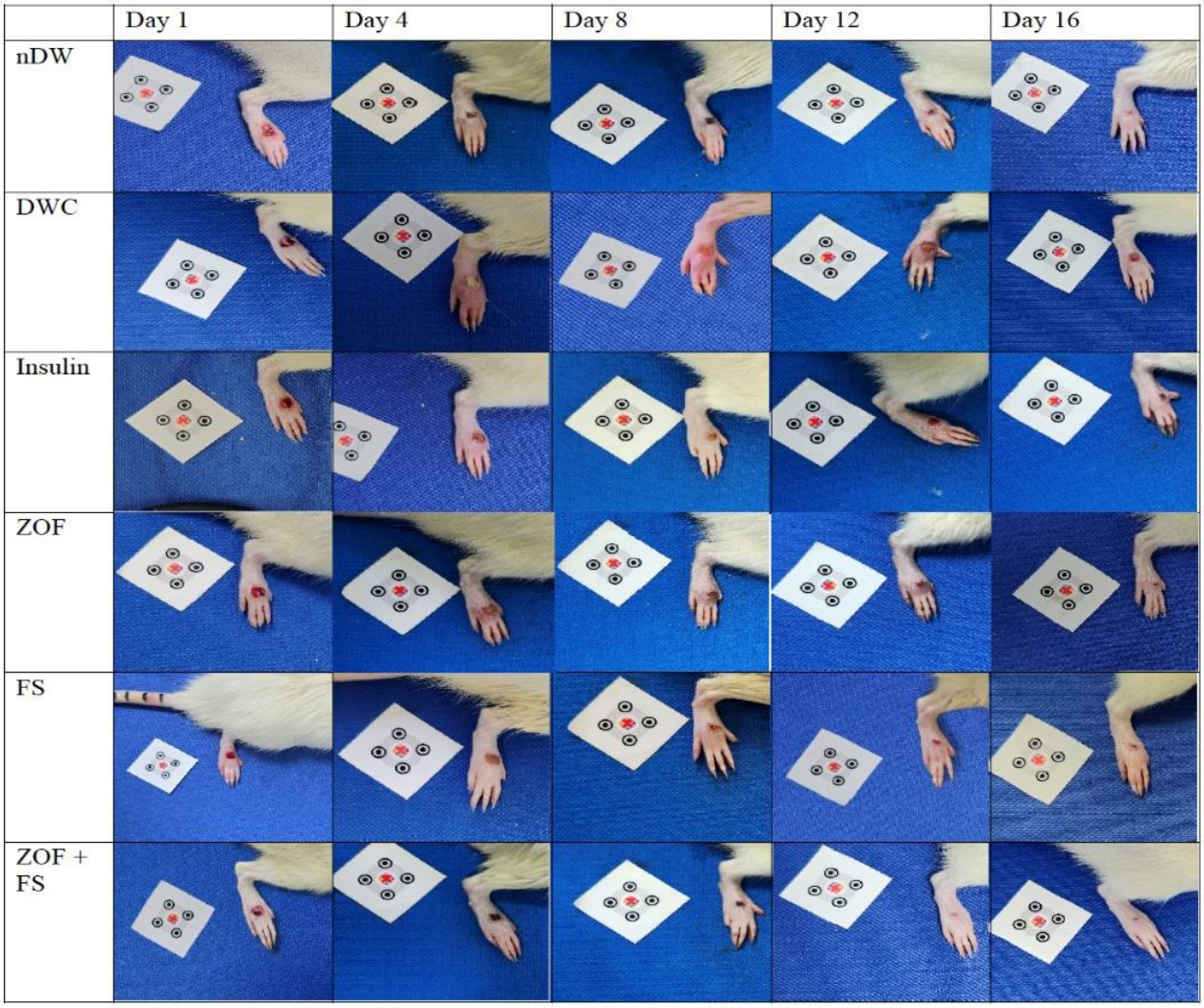

Figure 5: Morphological representation of rat hind paw with diabetic foot ulcer**.** Demonstrating different phases of wound healing on day 1,4,8,12,16. nDW: non-diabetic wounded. DWC: Diabetic Wounded Control, ZOF: Zofenopril, FS: Fisetin.

On Day 8, insulin (10 IU/kg), ZOF, FS, and their combination treatment significantly reduced the serum level of CRP ($p < 0.05$), and this level remained low on Day 16, showing a non-significant reduction in comparison with DWC ($p > 0.05$) (Figure 6A). Serum levels of IL-10 and TAOC were increased significantly ($p < 0.05$) in all STZ-induced diabetics on Day 1 (Figure 6B and C). Insulin resulted in a significant increase in TAOC on Days 8 and 16, no significant changes were observed in the ZOF, FS, and their combination on Day 8, while the IL-10 level was significantly decreased in the FS group on Day 16. A marked drop in the level of IL-10 is observed on Day 8 in the DWC, insulin, ZOF, FS, and their combination compared to the 1st day, and it is nearly comparable to the nDnW and nDW groups. On day 16, insulin resulted in a significant elevation in IL-10 compared to DWC. FS resulted in a significant decrease in IL-10, and ZOF+FS non-significantly increased the level of IL-10 (Figure 6D). Depicts serum levels of VEGF in different phases of wound healing in the presence of various treatment protocols. On Day 1 of post-wound induction, STZ resulted in a significant initial overproduction and elevation of serum level of VEGF ($p < 0.05$) in the early phase of wound healing. On Day 8, which is described as a proliferation phase, STZ resulted in a reduction of VEGF in DWC; however, insulin, ZOF, FS, and their combination nearly kept VEGF at a level higher than that of the DWC group, and the combined protocol of ZOF+FS shows significant elevation ($p < 0.05$) of VEGF level in this phase of wound healing. These effects continued to Day 16 in the same manner. In Figure 6E there was a significant decrease ($p < 0.05$) in serum level of hydroxyproline in rats in DWC compared with nDnW and nDW on Day 1 post-wound induction. However, treatment with insulin and FS resulted in the elevation of this biomarker in a significant manner ($p < 0.05$) on Day 8 and continued on Day 16. By Day 16, both the ZOF and insulin-treated groups demonstrated additional increases in hydroxyproline.

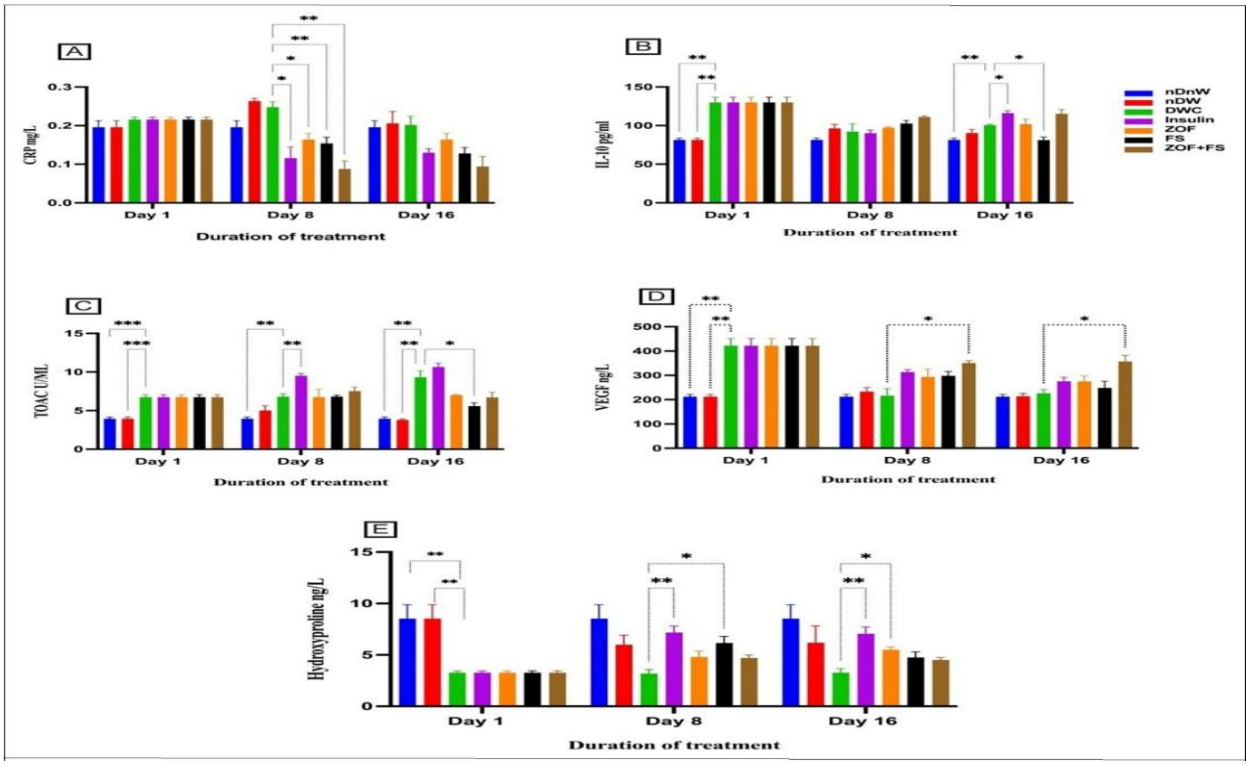

Figure 6: Effect of zofenopril and fisetin alone or in combination on serum level; **A**) CRP, **B**) IL-10, **C**) TAOC, **D**) VEGF, and **E**) Hydroxyproline in rats with diabetic foot ulcer. Data represented as mean±SEM, n=5. Data was analyzed using Two-way ANOVA followed by Dunnett's test. In **A**: CRP Day 1: Day 8: **p*<0.027 when comparing DWC *vs*. Insulin and ZOF; ***p*<0.0016 when comparing DWC *vs*. FS and ZOF+FS. In **B**: IL-10 Day 1: ***p*<0.0046 when comparing DWC *vs*. nDnW and nDW; Day 16: **p*<0.028 when comparing DWC *vs*. Insulin and FS, ***p*<0.0016 when comparing DWC *vs*. nDnW. In **C**: TOAC Day 1: ****p*=0.0008 when comparing DWC vs nDnW and nDW; Day 8: ***p*<0.003 when comparing DWC *vs*. nDnW and Insulin., Day 16: **p*<0.03 when comparing DWC *vs*. FS; ***p*<0.0094 when comparing DWC *vs*. nDnW and nDW. In **D**: VEGF Day 1: ***p*=0.0047 when comparing DWC vs nDnW and nDW; Day 8: **p*=0.03 when comparing DWC *vs*. ZOF+FS; Day 16: **p*=0.015 when comparing DWC *vs*. ZOF+FS. In **E**: Hydroxyproline Day 1: *p*** <0.005 when comparing DWC *vs*. nDnW, nDW; Day 8: **p*=0.02 when comparing DWC *vs*. FS; ***p*=0.005 when comparing DWC *vs*. Insulin; Day 16: **p*=0.01 when comparing DWC *vs*. ZOF, ***p*=0.007 when comparing DWC *vs*. Insulin. nDnW: non-diabetic, non-wounded; nDW: non-diabetic-wounded; DWC: diabetic wounded control; ZOF: zofenopril; FS: fisetin.

A histopathological morphometric quantitative assessment, including grading and scoring for various treatment groups, is shown in Table 1. All values, based on semi-quantitative histomorphologic analysis, are presented as mean percentages ± standard deviation (SD) for each parameter of angiogenesis, chronic inflammatory cell infiltration, and fibroblast proliferation in each group. The corresponding scores and grading for Day 8 are shown in Table 1. Additionally, histopathological micrographs stained with H&E are presented in Figure 7. It shows skin healing progression at three points: Day 1, Day 8, and Day 16, across the different treatment groups. Furthermore, the histopathological analysis of epidermal thickness revealed that the nDW group showed active epithelial cell proliferation on Day 8. By Day 16, the thickness decreased but remained thicker than normal, indicating proper remodeling. The DWC group had inactive epithelial proliferation on Day 8, and by Day 16, it showed poor remodeling and an unfavorable outcome. The treated groups (insulin, ZOF, and FS) showed active epithelial proliferation on Day 8, with remodeling occurring by Day 16, but the thickness still did not approach normal levels. In the ZOF+FS group, active fibroblast proliferation was observed on Day 8, and by Day 16, it showed excellent remodeling with thickness approaching normal skin levels. The corresponding scores and grading for each parameter of epidermal thickness and collagen deposition. Day 16 is shown in Table 2.

Table 1: Angiogenesis, inflammatory and fibroblast response

Groups	Day 8	Score	Grade	Day 16
Angiogenesis (%)				
nDnW	0±0.0^{a}	0	No	0±0.0^{a}
nDW	8.8±1.3^{b}	2	Moderate	1±0.7^{a}
DWC	3.8±0.83^{c}	1	Mild	23.4±1.4^{b}
Insulin	10.8±1.3^{d}	3	Marked	6±0.7^{c}
ZOF	11.6±1.14^{d}	3	Marked	1±0.7^{a,d}
FS	13.2±0.83^{d}	3	Marked	0±0.0^{a,d}
ZOF+FS	14.8±0.83^{d}	3	Marked	0±0.0^{a,d}
Chronic inflammatory cell infiltration (%)				
nDnW	0±0.0^{a}	0	No	0±0.0^{a}
nDW	39.4±1.14^{b}	2	Moderate	9.4±1.14^{b}
DWC	57.2±2.86^{c}	3	Severe	41.8±1.92^{c}
Insulin	36.2±1.92^{b}	2	Moderate	15.4±1.14^{d}
ZOF	31±1.87^{e}	2	Moderate	9±1.58^{b}
FS	37.8±1.92^{b}	2	Moderate	8.8±0.83^{b}
ZOF+FS	23.6±1.51^{f}	1	Mild	8.8±0.83^{b}
Fibroblast proliferation (%)				
nDnW	0±0.0^{a}	0	No	0±0.00^{a}
nDW	13.6±1.14^{b}	1	Mild	4±0.7^{b}
DWC	12±0.7^{b}	1	Mild	23.4±1.14^{c}
Insulin	16.6±1.14^{c}	2	Moderate	5.0±0.7^{b}
ZOF	24.8±0.83^{d}	2	Moderate	1.0±0.7^{a}
FS	25±1.0^{d}	3	Marked	0±0.0^{a}
ZOF+FS	32±1.58^{e}	3	Marked	0±0.0^{a}

The values are presented as mean±SD. Non-identical superscripts (a,b,c,d,e,f) represent significant differences between groups (one-way ANOVA) at $p<0.05$. n=5. nDnW: non-diabetic, non-wounded; nDW: non-diabetic-wounded; DWC: diabetic wounded control; ZOF: zofenopril; FS: fisetin.

Table 2: Epidermal thickness and collagen deposition

Groups	Day 8	Day 16	Score	Grade
Epidermal thickness (%)				
nDnW	2.28 ±0.5[a]	2.28±0.5[a]	1	Excellent
nDW	8.32±1.49[b]	4.71±0.29[b]	2	Proper
DWC	4.96±0.96[c]	6.55±1.25[c]	3	Poor
Insulin	6.23±2.30[c]	5.22±1.04[b]	3	Poor
ZOF	6.55±1.25[c]	4.55±1.24[c]	2	Proper
FS	7.40±1.83[c]	4.05±0.61[c]	2	Proper
ZOF+FS	10.37±2.53[d]	3.88±0.94[c]	1	Excellent
Collagen deposition (%)				
nDnW	52.52±1.81[a]	52.52±1.81[a]	3	Optimal
nDW	18.25±0.44[b]	29.56±0.59[b]	2	Moderate
DWC	14.15±0.87[c]	19.92±0.14[c]	1	Insufficient
Insulin	17.27±0.43[b]	31.09±0.74[b]	2	Moderate
ZOF	25.45±0.53[d]	37.22±1.18[d]	2	Moderate
FS	30.13±0.72[e]	41.08±1.24[e]	3	Optimal
ZOF+FS	32.77±1.04[f]	47.15±0.74[f]	3	Optimal

The values are presented as mean±SD. Non-identical superscripts (a,b,c,d,f) represent significant differences between groups (one-way ANOVA) at $p<0.05$. n = 5. nDnW: non-diabetic, non-wounded; nDW: non-diabetic-wounded; DWC: diabetic wounded control; ZOF: zofenopril; FS: fisetin.

Collagen deposition, stained with Masson's trichrome, is shown in Figure 8.

DISCUSSION

The regulation of blood glucose is a vital component of metabolic balance in diabetes. Therefore, this study emphasized the impact of ZOF and FS and their combination on blood glucose. The principal finding of this study is that ZOF and FS alone and in combination were able to significantly mitigate blood glucose levels in STZ-induced diabetes. As far as the available literature suggests, the effect of ZOF on diabetic control has not been adequately addressed in the previous studies [27]. A study on an isolated human pancreatic islet demonstrated that ACE inhibitors, particularly zofenoprilat, protect against high glucose exposure, as the study revealed that RAS molecules are present in human pancreatic islets, and their expression is regulated by glucose levels. Thus, the potential advantages of ACE inhibitors in diabetes are partly explained by their protective role in preserving pancreatic beta-cell function, with their beneficial effects associated with reduced oxidative stress [28]. Recent research indicates that ACE inhibitors may enhance insulin sensitivity and lower the risk of developing diabetes [29]. A meta-analysis comparing ACE inhibitors with ARBs found that ACE inhibitors were more effective in improving insulin sensitivity markers, including the insulin sensitivity index (ISI) composite, homeostasis model assessment of insulin resistance (HOMA-IR), the quantitative insulin sensitivity check index, and glucose infusion rate, particularly in hypertensive patients [12]. On the other hand, the effect of FS in the amelioration of glucose levels can be explained by the ability of the polyphenolic compounds in glycemic control and prevention of diabetic-associated complications [30]. Several studies reported a glucose-lowering effect of FS comparable to the current study, as FS possesses notable anti-diabetic and anti-inflammatory properties. Its oral administration for one month has been reported to decrease glycated hemoglobin (HbA1c), blood glucose levels, and the expression of gluconeogenic proteins while simultaneously increasing plasma insulin levels [31]. The finding of this study aligns with the previous research suggesting that FS exhibits pleiotropic effects, including antioxidant, anti-inflammatory, antimicrobial, and anti-diabetic [16], which contribute to the facilitation of the wound healing process. Although ZOF, FS, and their combinations affected glucose levels, their impact on body weight remains distinct and requires further analysis. In rats, when STZ-induced type 1 diabetes causes loss of body weight due to the depletion of adipose and muscle tissues, despite enhanced food and water consumption as well as intestinal growth [32]. Notably, in the present study, insulin administration led to weight reduction, consistent with previous studies that linked insulin therapy to body weight reduction in diabetic models due to enhanced glucose uptake and metabolic alteration [33]. Another study revealed that insulin lowers body weight by modulating hypothalamic signaling pathways, leading to a reduction in neuropeptide Y and galanin activity [34]. On the other hand, FS and ZOF+FS had no significant impact on body weight despite promoting wound healing, suggesting a potential protective role of FS against diabetes-induced catabolism. Furthermore, FS contributes to glucose homeostasis by regulating carbohydrate metabolism enzymes in STZ-induced diabetic rats [35]. Additionally, Maher et al. showed that FS possesses insulin-sensitizing characteristics, leading to improved glucose utilization and reduced muscle protein breakdown in diabetic mice [36]. In diabetes, one of the signaling pathways modulated by hyperglycemia is NF-κB-IKK-IKB, which normally controls the survival of B-cells; this pathway changes in diabetes toward increased expression of NF-κB, oxidative stress, and pro-inflammatory cytokines [37]. Therefore, in the other part of our investigation, the effects of ZOF, FS, and their combination on oxidative status and the inflammatory process were analyzed. The results showed a fluctuation in the animal's antioxidant system, specifically the serum level of IL-10 and TAOC in ZOF, FS, and their combination groups in different phases of the wound healing process, with a significant reduction in CRP level on Day 8. Initially, STZ administration resulted in a significant increase in the serum level of both IL-10 and TAOC in all STZ-induced diabetics on Day 1, followed by a marked reduction in the level of IL-10 and elevation in TAOC level in the proliferative phase in all treated groups. In the final phase of wound healing, FS resulted in a significant decrease in IL-10, whereas ZOF+FS non-significantly increased the level of IL-10; no significant changes were observed in the ZOF-treated group. The paradoxical elevation of antioxidant capacity in the early phase of wound healing in this experiment can be explained by the complex relationship between IL-10 and diabetes due to possessing both anti-inflammatory and inflammatory properties [38].

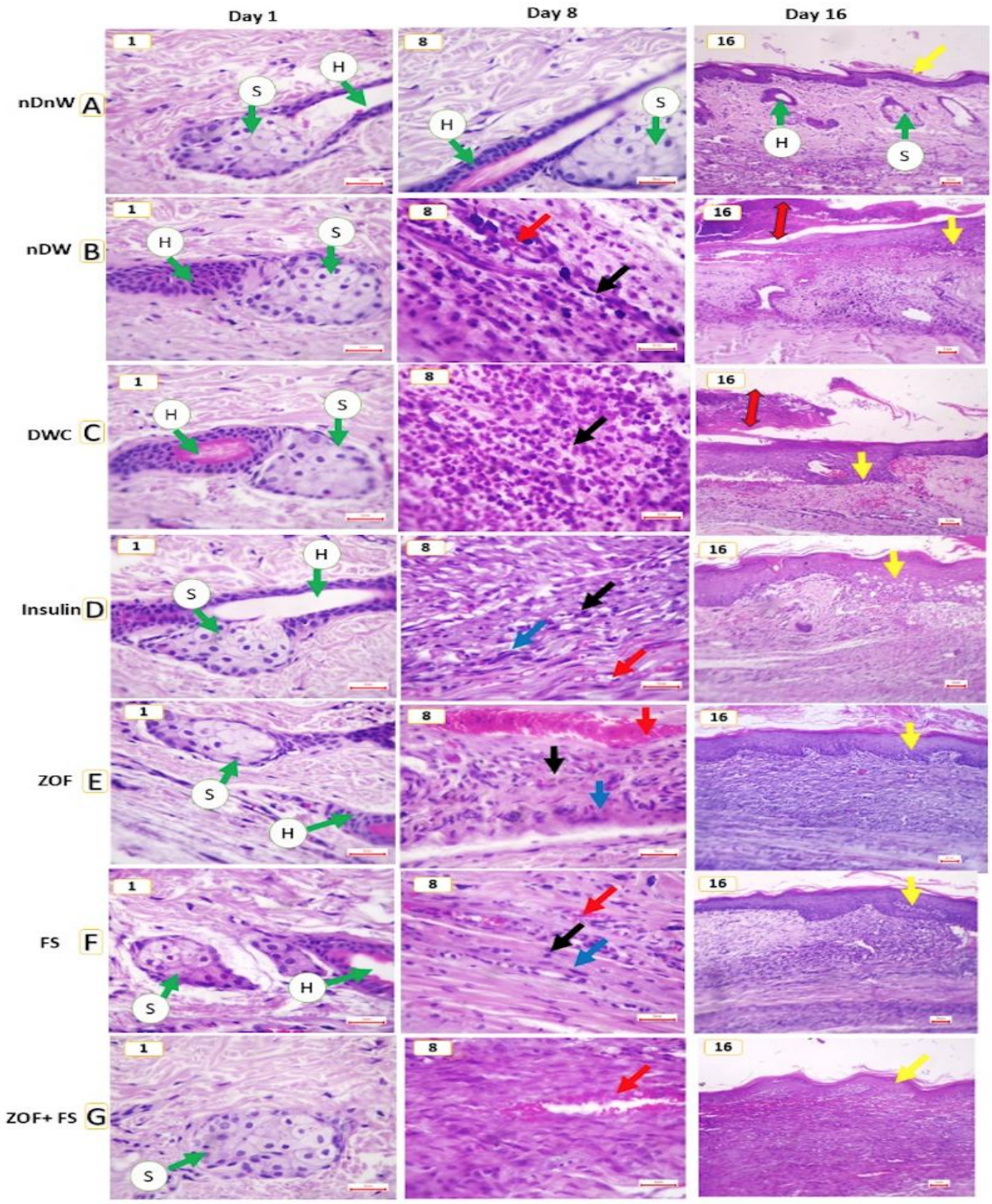

Figure 7: Photomicrograph of skin from all groups stained with hematoxylin and eosin (H&E). It illustrates the histological progression of skin healing at three-time points Day 1, Day 8, and Day 16 across different experimental groups. On Day 1, normal skin architecture is preserved in all groups, with the dermis containing hair follicles (H) and sebaceous glands (S). In Panel **A**, the non-diabetic, non-wounded (nDnW) group displays intact skin on both Day 8 and Day 16, with a thin epidermal layer maintaining normal histological characteristics by the final time point. Panel **B** shows the non-diabetic wounded (nDW) group, which exhibits moderate angiogenesis and inflammatory cell infiltration (score 2), with mild fibroblast presence (score 1) on Day 8. By Day 16, the nDW group demonstrates poor healing outcomes, with epidermal irregularities and protrusion toward the healed area. Panel **C** shows the diabetic wound control (DWC) group, which exhibits severe inflammatory cell infiltration (score 3) on Day 8, with mild angiogenesis and fibroblast activity. By Day 16, DWC still shows poor healing, with irregular epidermal thickness and persistent scab coverage. Panel **D** presents the insulin-treated group, Panel **E** the ZOF group, and Panel **F** the FS group, all exhibiting moderate angiogenesis and inflammatory cell infiltration on Day 8. By Day 16, these groups demonstrate moderate healing outcomes (score 2), with moderately regular epidermal layers, less protrusion, and moderately thin epidermis. Panel G illustrates the ZOF+FS-treated group, which exhibits mild inflammatory cell infiltration on Day 8, but with marked angiogenesis and fibroblast proliferation. By Day 16, this group achieves excellent healing outcomes (score 1), with a regenerated epidermis resembling normal skin and minimal protrusion toward the healed area. Throughout the sections, color-coded arrows highlight key histological features: yellow arrows indicate regenerated epidermis, bi-headed arrows denote the remaining scab, red arrows point to angiogenesis, black arrows highlight inflammatory cells, and blue arrows mark active fibroblasts. All images were stained with H&E, with observations on day 1 and day 8 made at 400X magnification, and day 16 images captured at 100x magnification (scale bar = 5 µm).

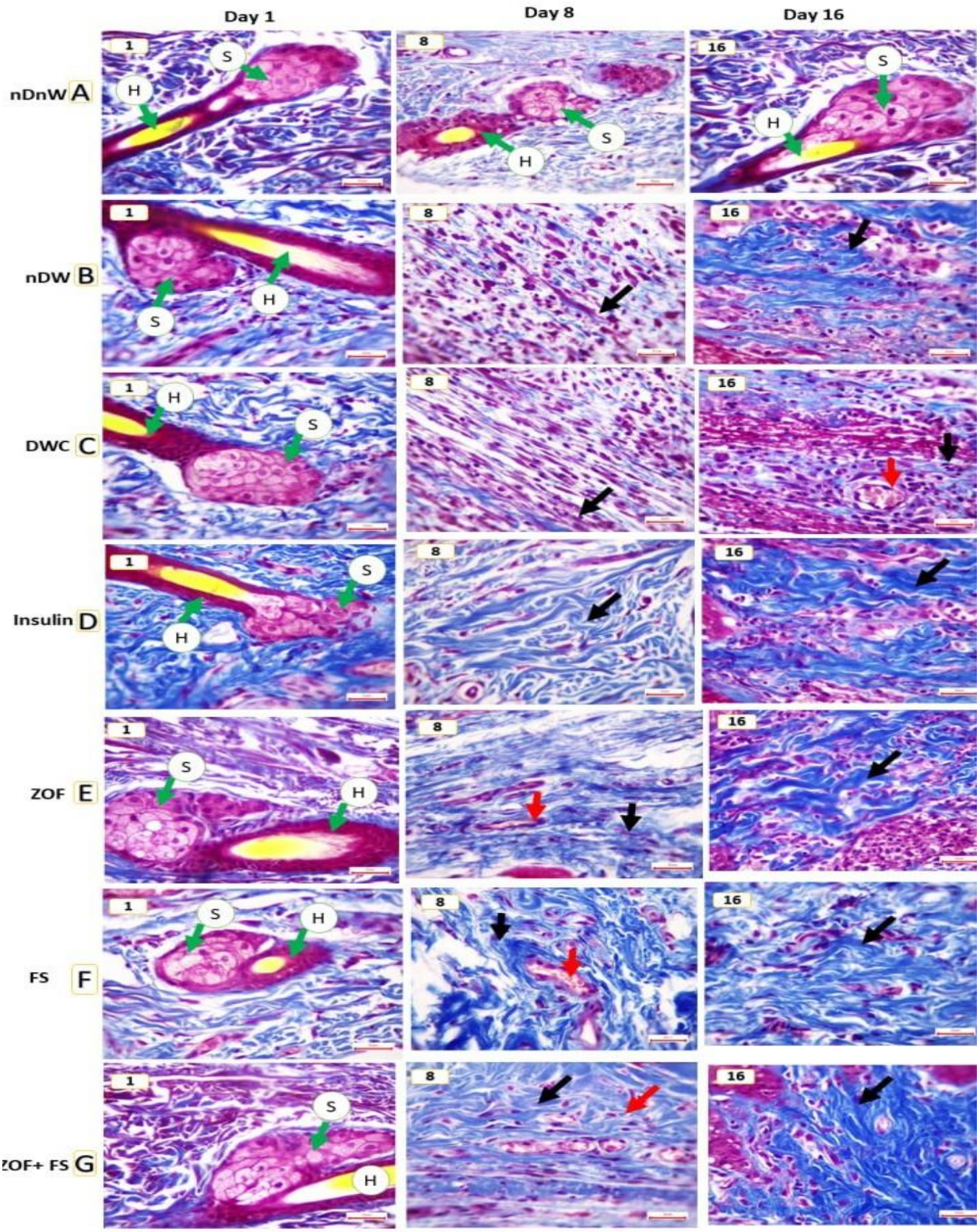

Figure 8. Photomicrograph of skin from all groups using Masson's trichrome staining**.** It illustrates the wound healing process on Day 1, Day 8, and Day 16, using Masson's trichrome staining to assess collagen deposition across all groups. On Day 1, the histological structure of normal skin is preserved, with the dermis containing hair follicles (H) and sebaceous glands (S). Panel **A** depicts the non-diabetic, non-wounded (nDnW) group, showing normal skin with collagen deposition and intact skin appendages, including sebaceous glands (S) and hair follicle shafts (H) on both Day 8 and Day 16. Panel **B** presents the non-diabetic wounded (nDW) group, which exhibits moderate fibroblast proliferation and mild, blue-colored collagen deposition on Day 8, progressing to moderate collagen deposition (score 2) with scattered inflammatory cells and active fibroblasts by Day 16. Panel **C** shows the diabetic wound control (DWC) group, demonstrating moderate fibroblast proliferation with mild collagen deposition on Day 8, but exhibiting insufficient collagen deposition (score 1), sustained angiogenesis (red arrow), and severe chronic inflammatory cell infiltration by Day 16. Panel **D** represents the insulin-treated group, while Panel **E** shows the ZOF-treated group. Both groups display moderate fibroblast proliferation and collagen deposition on Day 8, with improved collagen deposition and no significant inflammatory cell infiltration by Day 16. Panel **F** illustrates the FS-treated group, and Panel **G** depicts the ZOF+FS-treated group. Both groups exhibit moderate fibroblast proliferation with blue-colored collagen deposition on Day 8. By Day 16, these groups achieve optimal collagen deposition (score 3), with no remaining inflammatory cells and only a few active fibroblasts, indicating enhanced wound healing. Notably, angiogenesis is significantly reduced across all treated groups by Day 16. Throughout the sections, black arrows indicate fibroblast proliferation, while red arrows highlight angiogenesis. All images were stained with Masson's trichrome. Observations were made at 400× magnification, with a scale bar of 5 µm.

The STZ-induced oxidative stress stimulates the production of endogenous antioxidants as a compensatory response to excessive reactive oxygen species (ROS) [39]. To counteract these reactive species overproductions, the body upregulates enzymatic antioxidants such as superoxide dismutase, catalase, and glutathione peroxidase, along with non-enzymatic antioxidants like glutathione, uric acid, and albumin. Additionally, STZ-induced oxidative stress activates nuclear factor erythroid 2-related factor 2 (Nrf2), which promotes the expression of antioxidant defense enzymes, enhancing cellular protection against oxidative damage [40]. However, TAOC investigation revealed no significant changes in the serum level of TAOC in ZOF, FS, and their combination in the proliferative phase, while the TAOC level is significantly decreased in the FS group, and no changes have been observed in the ZOF group in the remodeling phase. This finding is inconsistent with the most recent study that highlighted the anti-inflammatory and antioxidant value of ZOF in the amelioration of cyclophosphamide-induced urotoxicity and nephrotoxicity [14]. Moreover, the two principal biomarkers linked to wound healing are VEGF and hydroxyproline. VEGF is a potent regulator of angiogenesis, facilitating the formation of blood vessels and enhancing the delivery of oxygen and nutrients to the wound site. It has a crucial role in wound healing by enhancing angiogenesis and vascular permeability to allow immune cells, nutrients, and oxygen to reach the site of the wound; these actions are necessary for the inflammatory and proliferative phases of wound healing [4]. One of the factors that facilitates these actions is VEGF, which concomitantly contributes to the development of granulation tissue, wound closure, and re-epithelialization. In this study, STZ-induced diabetes resulted in initial upregulation and overexpression of VEGF; this overexpression has been observed in many studies that highlighted the diabetic-associated complications [41,42]. This study assessed the serum level of VEGF as an indicative biomarker of proliferative and remodeling phases. The principal finding of this study revealed an initial elevation of VEGF levels observed on Day 1 of post-wound induction, followed by mild fluctuations and sustained levels in all treated groups (ZOF, FS, and ZOF+FS) by Day 8, while a noticeable reduction was observed in the DWC group in comparison to Day 1. VEGF plays a crucial role in facilitating fibroblast cell migration, triggering key mechanisms of the wound healing cascade, including angiogenesis, collagen synthesis, and epithelialization [43]. Therefore, sustaining VEGF levels by the treatments in this study provides evidence for a suggested mechanism of action of the treatments, particularly FS, in enhancing wound healing through transient upregulation of VEGF in fibroblasts and its proangiogenic effect that accelerates angiogenesis in the proliferative phase of wound healing. This finding can be supported by a recent study that focuses on the role of VEGF overexpression in fibroblast cells to increase angiogenesis and accelerate granulation tissue formation during the initial phase of wound healing [44]. To be pointed out, the antiangiogenic effect of FS is well-established, particularly in the context of diabetic retinopathy and cancer [45,46], as FS inhibits angiogenesis in diabetic retinopathy by suppressing VEGF expression [18]. However, in the wound healing process, FS might favor the proangiogenic effect in facilitating the healing of the wound. On the other hand, the effect of ZOF concerning enhancing angiogenesis in the proliferative and maturation phase of wound healing can be supported by earlier findings that demonstrated the proangiogenic effect of the ACE inhibitor perindopril in an animal model with induced hindlimb ischemia in a mechanism independent of the VEGF pathway [47]. Moreover, a recent study indicates that perindopril may be preferred over captopril for hypertensive individuals engaged in aerobic physical exercises because it does not inhibit the angiogenesis stimulated by aerobic training in skeletal and cardiac muscles [48]. Furthermore, hydroxyproline level serves as an indicator for collagen concentration, with higher hydroxyproline levels reflecting an accelerated wound healing process [49]. In this study, FS and ZOF elevated hydroxyproline levels significantly similar to insulin in the proliferative and remodeling phases of wound healing. Administering ZOF and FS to animals with the DFU model resulted in reduced inflammatory infiltration at the wound site, as evidenced by histopathological analysis, which could further boost collagen synthesis. Semiquantitative histological analysis revealed marked angiogenesis and fibroblast proliferation by ZOF, FS, and their combinations on Day 8 and moderate to excellent epidermal thickness with optimal collagen deposition on Day 16. The findings suggest that ZOF promotes collagen deposition by elevation of VEGF, thereby accelerating wound contraction and improving delayed wound healing in diabetes. The finding of our study is consistent with the results reported by Elloumi *et al*., which stated that flavonoids such as quercetin and myricetin have the potential to promote wound healing through stimulating collagen synthesis, indicated by elevated hydroxyproline levels in wound tissues. They also exhibit antibacterial and antioxidant activities, accelerating wound closure and regulating hydroxyproline concentration; they promote collagen production, as indicated by elevated hydroxyproline levels in wound tissues [50]. Further research is necessary to examine the molecular mechanism of ZOF and FS in diabetic foot ulcers, with a focus on their effects on other biomarkers of inflammation, oxidative stress, and angiogenesis.

Limitation of the study

This study has certain limitations. Firstly, the doses of ZOF and FS were selected based on existing literature, and no dose-response study was applied. Secondly, an assessment of additional novel biomarkers is required. A significant strong point of this study is the utilization of the ImitoWound application as an image analyzer for accurate wound evaluation. To the best of our knowledge, no prior

research on their effects exists. This study is the first to examine the impact of ZOF and FS on a diabetic wound model. It establishes a basis for further investigation and possible clinical applications in the treatment of diabetic foot ulcers.

Conclusion

Oral administration of ZOF, FS, and their combination enhanced wound restoration by ameliorating inflammation, improving angiogenesis, collagen synthesis, and re-epithelization in STZ-induced diabetic rats. The suggested mechanisms are anti-inflammatory, enhanced angiogenesis, and collagen synthesis via elevation of the level of VEGF and hydroxyproline, respectively, in addition to glycemic control, thereby accelerating wound contraction and improving delayed wound healing in diabetes. Improvement in the histopathological outcome of the DFU at different time points was aligned with the biochemical and morphological assessment of the wounds.

ACKNOWLEDGMENTS

The authors thank the College of Pharmacy, University of Sulaimani for the logistic support. The presented data were abstracted from MSc thesis submitted by Sozan Kamaran AbdulRazaaq to the Department of Pharmacology and Toxicology, College of Pharmacy, University of Sulaimani.

Conflict of interests

The authors declared no conflict of interest.

Funding source

The authors did not receive any source of funds.

Data sharing statement

Supplementary data can be shared with the corresponding author upon reasonable request.

REFERENCE

1. Wallace HA, Basehore BM, Zito PM, (Eds.), Wound Healing Phases. In: StatPearls. StatPearls Publishing; 2024. Accessed August 27, 2024. PMID: 29262065.
2. Rodrigues M, Kosaric N, Bonham CA, Gurtner GC. Wound healing: A cellular perspective. *Physiol Rev*. 2019;99(1):665-706. doi: 10.1152/physrev.00067.2017.
3. Nosrati H, Aramideh Khouy R, Nosrati A, Khodaei M, Banitalebi-Dehkordi M, Ashrafi-Dehkordi K, et al. Nanocomposite scaffolds for accelerating chronic wound healing by enhancing angiogenesis. *J Nanobiotechnology*. 2021;19(1):1. doi: 10.1186/s12951-020-00755-7.
4. Johnson KE, Wilgus TA. Vascular endothelial growth factor and angiogenesis in the regulation of cutaneous wound repair. *Adv Wound Care*. 2014;3(10):647-661. doi: 10.1089/wound.2013.0517.
5. Wong RSY, Tan T, Pang ASR, Srinivasan DK. The role of cytokines in wound healing: from mechanistic insights to therapeutic applications. *Explor Immunol*. 2025;5:1003183. doi: 10.37349/ei.2025.1003183.
6. Alamshah SM, Hemmati A, Nazari Z. Assessment of hydroxyproline levels in non-ischemic diabetic foot ulcers during recovery. A prospective case-control study. *Romanian J Diabetes Nutr Metab Dis*. 2015;22(4):361-366. doi: 10.1515/rjdnmd-2015-0042.
7. Silva IMS, Assersen KB, Willadsen NN, Jepsen J, Artuc M, Steckelings UM. The role of the renin-angiotensin system in skin physiology and pathophysiology. *Exp Dermatol*. 2020;29(9):891-901. doi: 10.1111/exd.14159.
8. Scholzen TE, Ständer S, Riemann H, Brzoska T, Luger TA. Modulation of cutaneous inflammation by angiotensin-converting enzyme. *J Immunol*. 2003;170(7):3866-3873. doi: 10.4049/jimmunol.170.7.3866.
9. Hedayatyanfard K, Khalili A, Karim H, Nooraei S, Khosravi E, Sadat Haddadi N, et al. Potential use of angiotensin receptor blockers in skin pathologies. *Iran J Basic Med Sci*. 2023;26(7). doi: 10.22038/ijbms.2023.66563.14606.
10. Bernasconi R, Nyström A. Balance and circumstance: The renin angiotensin system in wound healing and fibrosis. *Cell Signal*. 2018;51:34-46. doi: 10.1016/j.cellsig.2018.07.011.
11. Donnelly R. Angiotensin-converting enzyme inhibitors and insulin sensitivity: Metabolic effects in hypertension, diabetes, and heart failure: *J Cardiovasc Pharmacol*. 1992;20(Supplement 11):S38-S44. doi: 10.1097/00005344-199200111-00007.
12. Yao J, Fan S, Shi X, Gong X, Zhao J, Fan G. Angiotensin-converting enzyme inhibitors versus angiotensin II receptor blockers on insulin sensitivity in hypertensive patients: A meta-analysis of randomized controlled trials. Li Y, ed. *PloS One*. 2021;16(7):e0253492. doi: 10.1371/journal.pone.0253492.
13. Perkins JM, Davis SN. The renin–angiotensin–aldosterone system: a pivotal role in insulin sensitivity and glycemic control. *Curr Opin Endocrinol Diabetes Obes*. 2008;15(2):147-152. doi: 10.1097/MED.0b013e3282f7026f.
14. Mahmood N, Rashid B, Abdulla S, Marouf B, Hamaamin K, Othman H. Effects of zofenopril and thymoquinone in cyclophosphamide-induced urotoxicity and nephrotoxicity in rats; The value of their anti-Inflammatory and antioxidant properties. *J Inflamm Res*. 2025;18:3657-3676. doi: 10.2147/JIR.S500375.
15. Mustafa HH, Marouf BH, Muhamad SA, Hama Saeed DA, Ismaeel DO. Topically applied glycerol-based turmeric extract formulation ameliorates diabetic foot ulcer: A case report. *Al-Rafidain J Med Sci*. 2025;8(1):62-65. doi: 10.54133/ajms.v8i1.1649.
16. Antika LD, Dewi RM. Pharmacological aspects of fisetin. *Asian Pac J Trop Biomed*. 2021;11(1):1-9. doi: 10.4103/2221-1691.300726.
17. Dong W, Jia C, Li J, Zhou Y, Luo Y, Liu J, et al. Fisetin attenuates diabetic nephropathy-induced podocyte injury by inhibiting NLRP3 inflammasome. *Front Pharmacol*. 2022;13:783706. doi: 10.3389/fphar.2022.783706.
18. Lai M, Lan C, Zhong J, Wu L, Lin C. Fisetin prevents angiogenesis in diabetic retinopathy by downregulating VEGF. *J Ophthalmol*. 2023;2023:7951928. doi: 10.1155/2023/7951928.
19. Goodyear MDE, Krleza-Jeric K, Lemmens T. The Declaration of Helsinki. *BMJ*. 2007;335(7621):624-625. doi: 10.1136/bmj.39339.610000.BE.
20. Pengzong Z, Yuanmin L, Xiaoming X, Shang D, Wei X, Zhigang L, et al. Wound healing potential of the standardized extract of *Boswellia serrata* on experimental diabetic foot ulcer via inhibition of inflammatory, angiogenetic and apoptotic markers. *Planta Med*. 2019;85(08):657-669. doi: 10.1055/a-0881-3000.
21. Lau TW, Sahota DS, Lau CH, Chan CM, Lam FC, Ho YY, et al. An in vivo investigation on the wound-healing effect of two medicinal herbs using an animal model with foot ulcer. *Eur Surg Res*. 2008;41(1):15-23. doi: 10.1159/000122834.
22. Aarts P, Van Huijstee JC, Ragamin A, Reeves JL, Van Montfrans C, Van Der Zee HH, et al. Validity and reliability of two digital wound measurement tools after surgery in patients with hidradenitis suppurativa. *Dermatology*. 2023;239(1):99-108. doi: 10.1159/000525844.
23. Biagioni RB, Carvalho BV, Manzioni R, Matielo MF, Brochado Neto FC, Sacilotto R. Smartphone application for wound area measurement in clinical practice. *J Vasc Surg Cases Innov Tech*. 2021;7(2):258-261. doi: 10.1016/j.jvscit.2021.02.008.
24. Altunoluk B, Söylemez H, Bakan V, Ciralik H, Tolun FI. Protective effects of zofenopril on testicular torsion and detorsion injury in rats. *Urol J*. 2011;8(4):313-319.
25. Alikatte K, Palle S, Rajendra Kumar J, Pathakala N. Fisetin improved rotenone-induced behavioral deficits, oxidative changes, and mitochondrial dysfunctions in rat model of

Parkinson's disease. *J Diet Suppl*. 2021;18(1):57-71. doi: 10.1080/19390211.2019.1710646.
26. Cui J, Fan J, Li H, Zhang J, Tong J. Neuroprotective potential of fisetin in an experimental model of spinal cord injury: via modulation of NF-κB/IκBα pathway. *Neuroreport*. 2021;32(4):296-305. doi: 10.1097/WNR.0000000000001596.
27. Borghi C, Omboni S. Angiotensin-converting enzyme inhibition: Beyond blood pressure control—The role of zofenopril. *Adv Ther*. 2020;37(10):4068-4085. doi: 10.1007/s12325-020-01455-2.
28. Lupi R, Guerra SD, Bugliani M, Boggi U, Mosca F, Torri S, et al. The direct effects of the angiotensin-converting enzyme inhibitors, zofenoprilat and enalaprilat, on isolated human pancreatic islets. *Eur J Endocrinol*. 2006;154(2):355-361. doi: 10.1530/eje.1.02086.
29. Shin J, Kim H, Yim HW, Kim JH, Lee S, Kim H. Angiotensin-converting enzyme inhibitors versus angiotensin receptor blockers: New-onset diabetes mellitus stratified by statin use. *J Clin Pharm Ther*. 2022;47(1):97-103. doi: 10.1111/jcpt.13544.
30. Amin GSM, Marouf BH, Namiq HS, Salih JM. Impact of resveratrol and pharmaceutical care on type 2 diabetes mellitus and its neuropathic complication: A randomized placebo controlled clinical trial. *J Clin Pharm Ther*. 2024;2024(1):7739710. doi: 10.1155/2024/7739710.
31. Prasath GS, Pillai SI, Subramanian SP. Fisetin improves glucose homeostasis through the inhibition of gluconeogenic enzymes in hepatic tissues of streptozotocin induced diabetic rats. *Eur J Pharmacol*. 2014;740:248-254. doi: 10.1016/j.ejphar.2014.06.065.
32. Zafar M, Naeem-ul-Hassan Naqvi S. Effects of STZ-induced diabetes on the relative weights of kidney, liver and pancreas in albino rats: A comparative study. *Int J Morphol*. 2010;28(1). doi: 10.4067/S0717-95022010000100019.
33. Erdal N, Gürgül S, Demirel C, Yildiz A. The effect of insulin therapy on biomechanical deterioration of bone in streptozotocin (STZ)-induced type 1 diabetes mellitus in rats. *Diabetes Res Clin Pract*. 2012;97(3):461-467. doi: 10.1016/j.diabres.2012.03.005.
34. Park S, Hong SM, Ahn IS. Long-term intracerebroventricular infusion of insulin, but Not glucose, modulates body weight and hepatic insulin sensitivity by modifying the hypothalamic insulin signaling pathway in type 2 diabetic rats. *Neuroendocrinology*. 2009;89(4):387-399. doi: 10.1159/000197974.
35. Prasath GS, Subramanian SP. Modulatory effects of fisetin, a bioflavonoid, on hyperglycemia by attenuating the key enzymes of carbohydrate metabolism in hepatic and renal tissues in streptozotocin-induced diabetic rats. *Eur J Pharmacol*. 2011;668(3):492-496. doi: 10.1016/j.ejphar.2011.07.021.
36. Maher P, Dargusch R, Ehren JL, Okada S, Sharma K, Schubert D. Fisetin lowers methylglyoxal dependent protein glycation and limits the complications of diabetes. *PloS One*. 2011;6(6):e21226. doi: 10.1371/journal.pone.0021226.
37. AL-Ishaq RK, Abotaleb M, Kubatka P, Kajo K, Büsselberg D. Flavonoids and their anti-diabetic effects: Cellular mechanisms and effects to improve blood sugar levels. *Biomolecules*. 2019;9(9):430. doi: 10.3390/biom9090430.
38. Rios-Arce ND, Dagenais A, Feenstra D, Coughlin B, Kang HJ, Mohr S, et al. Loss of interleukin-10 exacerbates early Type-1 diabetes-induced bone loss. J Cell Physiol. 2020;235(3):2350-2365. doi:10.1002/jcp.29141.
39. Omar HM, Rosenblum JK, Sanders RA, Watkins JB. Streptozotocin may provide protection against subsequent oxidative stress of endotoxin or streptozotocin in rats. *J Biochem Mol Toxicol*. 1998;12(3):143-149. doi: 10.1002/(SICI)1099-0461(1998)12:3<143::AID-JBT2>3.0.CO;2-L.
40. Xu Z, Wei Y, Gong J, Cho H, Park JK, Sung ER, et al. NRF2 plays a protective role in diabetic retinopathy in mice. *Diabetologia*. 2014;57(1):204-213. doi: 10.1007/s00125-013-3093-8.
41. Cho CH, Roh KH, Lim NY, Park SJ, Park S, Kim HW. Role of the JAK/STAT pathway in a streptozotocin-induced diabetic retinopathy mouse model. *Graefes Arch Clin Exp Ophthalmol*. 2022;260(11):3553-3563. doi: 10.1007/s00417-022-05694-7.
42. Wu X, Yang Z, Li Z, Yang L, Wang X, Wang C, et al. Increased expression of hypoxia inducible factor-1 alpha and vascular endothelial growth factor is associated with diabetic gastroparesis. *BMC Gastroenterol*. 2020;20(1):216. doi: 10.1186/s12876-020-01368-y.
43. Veith AP, Henderson K, Spencer A, Sligar AD, Baker AB. Therapeutic strategies for enhancing angiogenesis in wound healing. *Adv Drug Deliv Rev*. 2019;146:97-125. doi: 10.1016/j.addr.2018.09.010.
44. Shams F, Moravvej H, Hosseinzadeh S, Mostafavi E, Bayat H, Kazemi B, et al. Overexpression of VEGF in dermal fibroblast cells accelerates the angiogenesis and wound healing function: in vitro and in vivo studies. *Sci Rep*. 2022;12(1):18529. doi: 10.1038/s41598-022-23304-8.
45. Zhou C, Huang Y, Nie S, Zhou S, Gao X, Chen G. Biological effects and mechanisms of fisetin in cancer: a promising anti-cancer agent. *Eur J Med Res*. 2023;28(1):297. doi: 10.1186/s40001-023-01271-8.
46. Bhat TA, Nambiar D, Pal A, Agarwal R, Singh RP. Fisetin inhibits various attributes of angiogenesis in vitro and in vivo--implications for angioprevention. *Carcinogenesis*. 2012;33(2):385-393. doi: 10.1093/carcin/bgr282.
47. Silvestre JS, Bergaya S, Tamarat R, Duriez M, Boulanger CM, Levy BI. Proangiogenic effect of angiotensin-converting enzyme inhibition is mediated by the bradykinin B2 receptor pathway. *Circ Res*. 2001;89(8):678-683. doi: 10.1161/hh2001.097691.
48. Macedo AG, Miotto DS, Tardelli LP, Santos CF, Amaral SL. Exercise-induced angiogenesis is attenuated by captopril but maintained under perindopril treatment in hypertensive rats. *Front Physiol*. 2023;14:1147525. doi: 10.3389/fphys.2023.1147525.
49. Dwivedi D, Dwivedi M, Malviya S, Singh V. Evaluation of wound healing, anti-microbial and antioxidant potential of Pongamia pinnata in wistar rats. *J Tradit Complement Med*. 2017;7(1):79-85. doi: 10.1016/j.jtcme.2015.12.002.
50. Elloumi W, Mahmoudi A, Ortiz S, Boutefnouchet S, Chamkha M, Sayadi S. Wound healing potential of quercetin-3-O-rhamnoside and myricetin-3-O-rhamnoside isolated from Pistacia lentiscus distilled leaves in rats model. *Biomed Pharmacother*. 2022;146:112574. doi: 10.1016/j.biopha.2021.112574.